

# A Partitioning Approach to RFID Identification

Jian Su, *Member, IEEE*, Alex X. Liu, *Fellow, IEEE*, Zhengguo Sheng, *Senior Member, IEEE* and Yongrui Chen, *Member, IEEE*

**Abstract**—Radio-frequency identification (RFID) is a major enabler of Internet of Things (IoT), and has been widely applied in tag-intensive environments. Tag collision arbitration is considered as a crucial issue of such RFID system. To enhance the reading performance of RFID, numerous anti-collision algorithms have been presented in previous literatures. However, most of them suffer from the slot efficiency bottleneck of 0.368. In this paper, we revisit the performance of tag identification in Aloha-based RFID anti-collision approaches from the perspective of time efficiency. Based on comprehensive reviews and analysis of the existing algorithms, a novel partitioning approach is proposed to maximize identification performance in framed slotted Aloha based UHF RFID systems. In the proposed approach, the tag set is divided into many groups which only contains a few tags, and then each group is identified in sequence. Benefiting from the optimal partition, the proposed algorithm can achieve a significant performance improvement. Simulation results supplemented by prototyping tests show that the proposed solution achieves an asymptotical slot efficiency up to 0.4348, outperforming the existing UHF RFID solutions.

**Index Terms**—RFID, anti-collision, Partitioning, time efficiency, experiments.

## 1 INTRODUCTION

### 1.1 Background And Problem Statement

Radio-frequency identification is a wireless communication technology that uses radio signals to identify target objects and obtain the corresponding information without mechanical or optical contact between the system and the target objects [1], [2]. Compared with manual systems such as barcodes, RFID has many advantages, such as, non-line of sight, multi-target identification, long lifetime, repeatable reading and writing, positioning and tracking. With the reduction of production costs, it has been widely used in supply chain monitoring, warehouse management, inventory control, food traceability, industrial automation and other fields [3]–[5]. In these applications, items are often labeled with miniaturized tags, each tag has a unique ID and can store private information of an item, which can be extracted by the back-end server for automated management of items.

According to IDtechEx's the latest forecast report, the total market value of RFID will reach 14.9 billion dollars by 2022 [6].

The RFID system can be divided into active, passive and semi-active according to the way that RFID tag is powered [7]. The energy required for active tag operation is completely provided by the built-in battery. The advantages of the active tag is that it has a long working distance, can sense the channel and detect collision. However, the disadvantage is that it is bulky and requires regular battery replacement, which is costly to use. Passive tag has no built-in battery and only works within the radiation field of the reader. The operation energy is provided by the electromagnetic waves sent by the reader. Therefore, its computational ability is limited, and it is impossible to sense the channel, detect collisions and communicate with other tags. Semi-passive tag behaves in a similar manner to passive tag, but has an extra on-board battery that powers its microchip. Passive RFID system is mostly used because its low-cost and convenience compared to active and semi-active RFID system [8].

This paper concerns the fundamental problem of passive RFID tag reading, i.e., reading all IDs of a given tag set. RFID tag reading is necessary and critical for all types of RFID systems. The tag reading process involves communication between the reader and multiple tags and takes place in a shared wireless channel [9]. Basically, the reader identifies tags nearby by broadcasting a probe command. The exact format of this command depends on the RFID standard specification. Tags are energized by the transmitted RF signal from the reader and respond to it with their IDs. When multiple tags simultaneously reply the reader, the signals will interfere with each other, causing collision among multiple tags [9]. To cope with the collision problem in RFID systems, the reader needs to adopt a certain strategy to coordinate the communication between the reader and tags. This strategy is called an anti-collision algorithm or protocol.

*Manuscript received March 25, 2019; revised January 21, 2020 and June 15, 2020; accepted June 19, 2020. This work is supported by the National Natural Science Foundation of China (No.61802196); the Natural Science Foundation of Jiangsu Province (No.BK20180791); This work is partially supported by the National Science Foundation under Grant Number CNS-1837146. This work is also supported in part by Soft Academic Program of China Meteorological Administration, the Priority Academic Program Development of Jiangsu Higher Education Institutions. This work is also supported in part by Engineering Research Center of Digital Forensics, Ministry of Education. The associate editor coordinating the review of this article and approving it for publication was Dr. M. Li. (Corresponding authors: Yongrui Chen; Zhengguo Sheng)*

*J. Su is with the School of Computer and Software, Nanjing University of Information Science and Technology, Jiangsu 210044, China (e-mail: sj890718@gmail.com).*

*Alex X. Liu is with Qilu University of Technology and Ant Financial Services Group, Shandong 250353, China (Email: alexliu360@gmail.com).*

*Z. Sheng is with the Department of Engineering and Design, University of Sussex, Brighton BN1 9RH, U.K. (e-mail: z.sheng@sussex.ac.uk).*

*Y. Chen is with the School of Electronic, Electrical, and Communication Engineering, University of Chinese Academy of Sciences, Beijing, 100190, P.R.China (e-mail: chenyr@ucas.ac.cn).*

*Digital Object Identifier xxxx*

Aloha-based algorithm was first developed for random access in packet radio networks. To optimize the reading performance of RFID systems, the dynamic framed slotted Aloha (DFSA) is developed and widely used in EPC C1 Gen2 UHF RFID standard. The work mechanism of DFSA is that the reader initializes the reading process by broadcasting a frame length  $F$  to the tags in its vicinity, where  $F$  corresponds to the number of time slots available per frame. Those tags that receive the parameter  $F$  randomly pick up a time slot and reply during that slot. For a given time slot, the reader can observe three outcomes: a singleton slot, an empty slot, and a collision slot. Only when the reader detects a singleton slot, it issues an Acknowledge command to obtain the ID from a tag. After reading a frame, the reader updates a new frame length according to the estimation of cardinality (i.e., the number of unread tags) and starts a new reading round.

The performance of DFSA depends on both the cardinality estimation and the setting of frame length. For a particular frame, the slot efficiency is defined as the number of singleton slots over the frame size. As the tag number increases, the maximum slot efficiency 0.368 can be achieved asymptotically [10]–[14] when the frame size is equal to the number of tags queried by the reader. The key limitations of Aloha-based solutions are three-fold. First of all, in the actual situation, the reader is unable to increase the frame size infinitely to fit the tag cardinality. The reason is that all of tags, containing those that have been successfully identified, need to stay powered up and to maintain the inventoried flags in Aloha-based protocols. Once some tags are intermittently powered down, their inventoried flags are reset and continue to participate in channel contention to affect the identification of the remaining tags, resulting in instability of the Aloha-based solutions. In addition, to improve the estimation accuracy, most previous algorithms incur high computational cost because they need to ensure the estimation accuracy. However, the anti-collision solutions with complex estimation are difficult to implement to low-cost reader (e.g. mobile or handheld reader) due to its constrained computational ability. Finally, the conventional DFSA algorithm suffers from a performance bottleneck of 0.368. Therefore, it is necessary to design an anti-collision approach with high time efficiency to address the above limitations.

## 1.2 System Model

Most tags and readers on the market are strictly complying with UHF RFID standards, especially following EPC C1 Gen2, i.e., Impinj, Alien, etc. A reasonable assumption is that the reader can be reprogrammed to update its firmware to support some custom commands without physical changes to either tags or the reader. To implement the proposed anti-collision algorithm in UHF RFID, we follow the EPC C1 Gen2 specification. Specifically, EPC C1 Gen2 specifies a series of commands for the reader, including Query, QueryAdj, QueryRep, and Ack, etc. The reader firstly initializes the identification process by broadcasting the Query command to the tags in its vicinity, and then schedules the identification process by alternative using QueryAdj and QueryRep. The Query command contains a dynamic

parameter  $Q$ , which is an integer from 0 to 15 and denotes the initial size of frame ( $F = 2^Q$ ). The QueryAdj command is used to update the parameter  $Q$ . After the receiving of Query command, each tag generates a 16-bit random number (called RN16) and extracts a  $Q$ -bit subset from RN16 as its slot counter  $SC$  ( $0 \leq SC \leq 2^Q - 1$ ). The value of tag slot counter ( $SC$ ) will be decreased by QueryRep command. When  $SC = 0$ , the tag will send its generated RN16. If a valid RN16 is detected, the reader will acknowledge with ACK command including the RN16. After successfully receiving the ACK, tags respond with their IDs, i.e., Electronic Product Code (EPC). When the EPC is correctly decoded, the reader will justify current time interval as a singleton slot. If more than one tag respond with their RN16s, the reader will justify current time interval as a collision slot and send a QueryRep command to proceed to the next slot. If no RN16 is detected, the reader will justify current time interval as an empty slot. After the reading of current frame, the reader starts a new identification round by using QueryAdj command. The duration of a time slot in DFSA is depending on the interrogation parameters between the reader and tags. Fig. 1 Introduces the timing details for each slot type in EPC C1 Gen2.

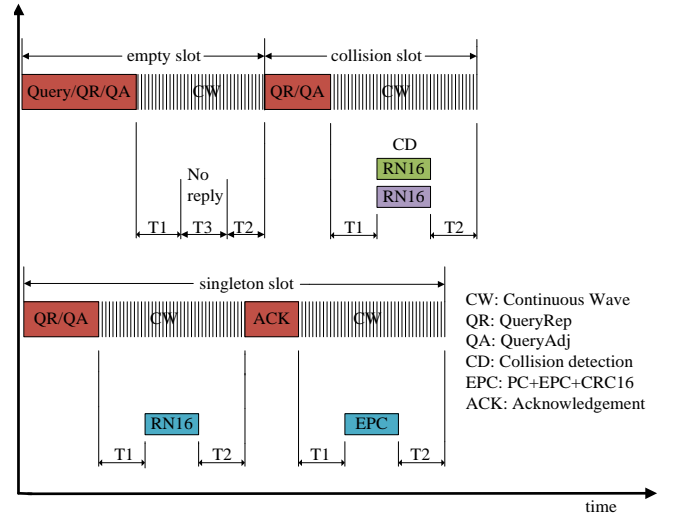


Fig. 1. The link timing between a reader and tags in EPC C1 Gen2

## 1.3 Proposed Solution

To address the fundamental limitations that lie in the randomness nature of prior Aloha-based algorithms, we propose an optimal partition based dynamic framed slotted Aloha (OP-DFSA). The key novelty of OP-DFSA is to formulate the multi-tag identification problem as a partitioning problem and find the optimal solution that ensures either minimal expectation of the number of slots or maximal expectation of time efficiency. In OP-DFSA, the cardinality of tag set is estimated based on the slot statistics observed in a sub-frame. Based on the estimated cardinality, the reader calculates the optimal number of partitioning to perform the identification phase so that the expected slot efficiency or expected time efficiency is maximal, and then performs individual identification phase (IIP) at each subset. After a subset is resolved, the IIP is performed to another subsets

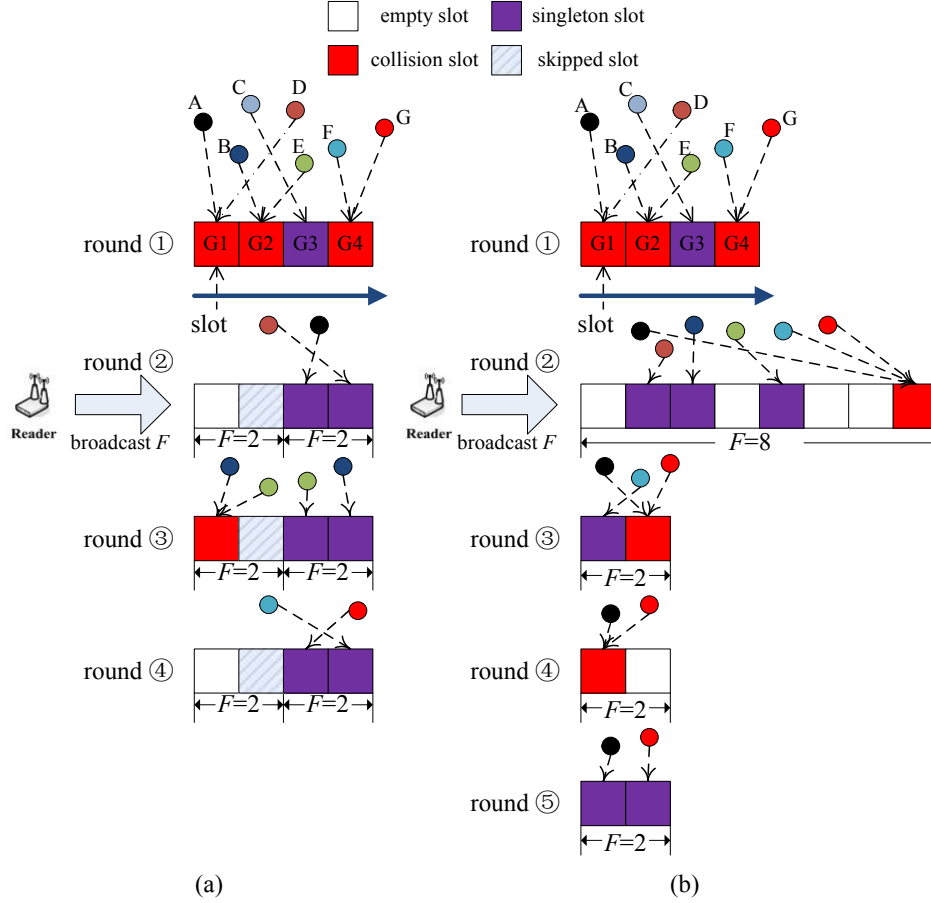


Fig. 2. Identifying seven tags using OP-DFSA and conventional DFSA: (a) tags identified by OP-DFSA (b) tags identified by conventional DFSA

until all subsets are resolved. To visually show the merits of the proposed solution, Fig. 2 gives an identification example of seven tags by using OP-DFSA and conventional DFSA, respectively, where a skipped slot means that the slot is hopped by the OP-DFSA during an identification process. As can be observed in Fig. 2 (a), the OP-DFSA consumes 16 slots to identify these seven tags. In comparison, the conventional DFSA consumes 18 slots to identify the same batch of tags as shown in Fig. 2 (b). This difference scales significantly as the number of tags increases.

#### 1.4 Summaries of Numerical Results

We evaluate the proposed OP-DFSA in MATLAB R2012b over extensive Monte Carlo simulations. The OP-DFSA significantly improves the reading performance over the existing DFSA algorithms. Simulation results supplemented to show that the proposed solution outperforms the best prior Aloha-based algorithms on the metrics of slot efficiency, time efficiency and tag identification rate by an average of 18.1%, 5.02%, and 5.24%, respectively, when the number of tags is from 5 to 95, and of 27.4%, 7.45%, and 7.69%, respectively, when the number of tags is from 100 to 1000. The reasons are as follows. The OP-DFSA makes full use of the partitioning feature to divide the entire tag set into several subset. For each subset, the IIP is elaborately designed to minimize the number of slots to identify the specific number of tags (especially when the number of tags is small),

thereby improving the overall slot efficiency. Both optimum partitioning and the designed IIP contribute to a significant improvement of performance. We also implemented OP-DFSA on a practical RFID system following the EPC C1 Gen2 UHF RFID standard, and evaluated it in an open environment. Our experimental results show that OP-DFSA consumes 165.5 milliseconds (ms) to read 20 tags under a low rate mode, improving average identification rate by 21.8% and 9.35% in comparison with Q-algorithm specified by the EPC C1 Gen2 and Impinj industrial solution.

## 2 RELATED WORKS

With consideration of cost and implementation complexity, the time-division multiple access (TDMA) approaches have been mainly used in RFID systems. That is, each tag monopolizes a channel in a separated time interval and communicates to the reader. We review the existing TDMA-based identification algorithms, which can be further divided into probabilistic [10], [11], [15]–[20], deterministic [21], or hybrid [22], [23].

### 2.1 Probabilistic Algorithms

Existing such algorithms are either Aloha-based [18] or tree splitting (TS)-based [17], which have been widely used in EPC C1 Gen2 or ISO/IEC 18000-6B. In BS, a collided tag set is continuously divided into smaller subsets by random

binary number. Although TS algorithm also belongs to a probabilistic algorithm, it is insensitive to tag cardinality because the splitting probability for collided tag set is constant to 0.5 regardless of tag cardinality. However, it has relatively long identification latency due to the large number of concurrent tags involved in each collision slot. Moreover, the tag ID is used for collision arbitration in TS solution, which increase the total collision arbitration time and reduce the time efficiency. Furthermore, TS algorithm is not compatible with EPC C1 Gen2. ABS and FSA-CSS are TS-based solutions that are designed for continuous identification of tags [17].

Compared to TS-based approaches, DFSA algorithm is more favored by EPC C1 Gen2. Most RFID manufacturers currently comply with the EPC C1 Gen2 standard, promoting the research of DFSA algorithms. As mentioned above, the DFSA algorithms with high computational complexity are not suitable for low-cost readers. Recently, many DFSA work has been presented to reduce computational overhead. In literature [24], a simple but relatively accurate method (FEIA) is proposed for tag cardinality. However, the estimation operation and frame size adjustment should be performed slot-by-slot, which causes a heavy loading for a computation-constrained reader. To reduce the estimation cost, an efficient anti-collision algorithm with early adjustment of frame length (EACAEA) is presented [25]. EACAEA is viewed as an improved version of FEIA. Since the estimation and frame size determination depends on one examination of a frame at a specific time slot during each identification round, it can achieve a good compromise between computational complexity and reading performance. The authors in [26] introduced an Improved Linearized Combinatorial Model (ILCM) to estimate the cardinality with modest calculation cost. However, its performance fluctuates sharply with the number of unread tags because the ILCM adopts a frame-by-frame (FbF) based cardinality estimation. To achieve the robust performance, the slot-by-slot (SbS) version of ILCM has been presented in [27]. The sub-frame based algorithms [28], [29] recently have been proposed to overcome the accumulated estimation error. Specifically, the tag cardinality is estimated based on linear relation between empty and collision slot statistically counted in a sub-frame [28]. Since the computational complexity of the estimation is reduced, the energy efficiency of SUBF-DFSA can be improved compared to the estimation methods with high complexity. However, since the usage of empirical correction is not based on theoretical calculation, the accuracy of estimation is not sufficient. In [29], a dynamic sub-frame based maximum a posteriori probability (DS-MAP) method is proposed to enhance the estimation accuracy and hence to improve the reading performance. To cease the estimation errors, the DS-MAP will return to conventional DFSA when it finds an appropriate frame. Although the sub-frame based algorithm can improve the reading performance, their slot efficiency still below the upper bound (among implementable EPC C1 Gen2-based algorithms) of 0.368. For the purpose of breaking the performance bottleneck of DFSA algorithms, a partition based anti-collision algorithm named detected sector based DFSA (ds-DFSA) is proposed [30]. The highest slot efficiency of ds-DFSA peaks at 0.41.

## 2.2 Deterministic Algorithms

A recent bit-tracking technology [31] which allows a reader to identify the locations of collided bit is proposed and widely used in the latest version of deterministic algorithm, i.e., query tree-based algorithm. For QT-based algorithm, every tag is assigned with a unique ID. The QT algorithm is working as a virtual depth-first traversal tree. The depth is defined as the number of branches from the root node to the leaf node. Each branch is marked with the method of “left 0 right 1”. The reader first queries the tags by using prefix 0, and the tags whose IDs start with 0 will transmit their IDs to the reader. If a collision occurs, the reader updates two new prefixes by appending a 0 and 1 at the end of the previous prefix and push them in the stack. The identification process is end then the stack is empty. The current research [32]–[36] on the QT-based algorithm focuses on how to use the collision information to update the query prefix. The literature [32] presented a collision tree (CT) algorithm which generates prefix and splits collided tags according to the first collided bit. STT improves the traditional QT using some ad hoc heuristics to update prefixes based on the previous response status [33]. M-ary query tree (MQT) has been proposed in [34], by forming a M-ary traversal tree instead of a binary tree for collided tags. In QwT [35], a window procedure is presented to manage the length of tags’ bit-stream to limit the energy wastage in collisions. The DPPS identifies two tags in a slot by sending two prefixes in a query string [36]. However, it is unable to detect the location of collision bit efficiently because of the wide deviation of backscatter link frequency of tags in a UHF RFID system [37]. Therefore, the algorithms embedded in bit-tracking technology are difficult to implement in UHF RFID systems.

## 2.3 Hybrid Algorithms

There are also hybrid [22], [23], [38] anti-collision algorithms that enhance the slot efficiency by combining the features of deterministic and probabilistic algorithms. There are two major types of such algorithms. MAS [22] is a QT-based algorithm embedded in the Aloha feature where each tag matches the prefix string and randomly chooses a slot from a frame to respond to the reader. For a large number of tags, the response in each slot of the frame is most likely a collision, which increases the identification latency. Furthermore, such algorithm also needs to introduce bit-tracking technology [38]. Hence, it is incompatible to the UHF RFID systems. Another representative named adaptive binary tree slotted Aloha (ABTSA) [23] has been proposed by incorporating merits of TS and Aloha-based algorithms. ABTSA uses TS-based algorithm to identify the collided tag set, which makes it incompatible with the EPC C1 Gen2 standard. Furthermore, identifying collided tags in TS manner is in itself very time-consuming.

## 3 ALGORITHM DESCRIPTION

### 3.1 OP-DFSA Overview

The proposed OP-DFSA algorithm contains two main phases: cardinality estimation phase and partitioning based identification phase. First, the reader can quickly obtains a tag

cardinality according to the estimation phase. Second, based on the estimated tag cardinality, the reader calculates the optimal number of subsets to start partitioning based identification phase so that the tag set is optimally partitioned to several subsets, and then perform individual identification phase on each subset. The individual identification phase will be introduced elaborately in Section 3.3. After a subset is successfully identified, the reader hops to the next subset and continue with the individual identification phase. This process continues until all tags are successfully identified.

### 3.2 Cardinality Estimation

As mentioned in section I the tag number is unknown in most application scenarios, the reader needs to estimate the cardinality to implement the corresponding anti-collision algorithm. To reduce the complexity cost during an estimation process, we adopts the Look-up Tables (LUTs) to pre-store intermediate variable of estimation results. The estimation function is referred to the maximum a posteriori probability (MAP) method to calculate the cardinality based on the feedbacks from a sub-frame. Restricted by the sub-frame size and the item quantity in the tables, the proposed estimation strategy is space-efficient and implementable. Considering  $n$  tags allocated in  $F$  slots, the probability that empty slot occurs  $e$  times, singleton slot occurs  $s$  times, and collision slot occurs  $c$  times in a sub-frame  $F_{sub}$  can be expressed as [29], [39]

$$P(F_{sub}, e, s, c) = \left( \frac{F_{sub}!}{e!s!c!} \right) P_0 P_1 P_2 \quad (1)$$

where  $P_0$ ,  $P_1$ , and  $P_2$  are the conditional probabilities of empty, singleton, and collision slot, can be calculated as

$$P_0 = \left( 1 - \frac{e}{F_{sub}} \right)^n \quad (2)$$

$$P_1 = \binom{n}{s} \left( \frac{s}{F_{sub}-e} \right)^s \left( 1 - \frac{s}{F_{sub}-e} \right)^{n-s} \frac{s!}{s^s} \quad (3)$$

$$= \binom{n}{s} \left( \frac{(F_{sub}-e-s)^{n-s}}{(F_{sub}-e)^n} \right) s!$$

$$P_2 = \sum_{k=0}^c \sum_{v=0}^{c-k} (-1)^{(k+v)} \binom{c}{k} \binom{c-k}{v} \quad (4)$$

$$\times \frac{(n-s)!}{(n-s-k)!} \frac{(c-k-v)^{(n-s-k)}}{c^{(n-s)}}$$

The tag cardinality involved in a sub-frame is determined when the value of  $P(n|e, s, c)$  is maximized. Therefore, the estimated result of tag cardinality in a sub-frame is  $\hat{n}_{sub}$ . Then the estimated cardinality involved in the full frame is calculated as

$$\hat{n}_{est} = \hat{n}_{sub} \times \frac{F}{F_{sub}} \quad (5)$$

To reduce computational complexity, the estimated results of tag cardinality during the sub-frame can be stored in the preset LUTs. Although the proposed estimation strategy requires additional storage space to store the LUTs, it can use the sub-frame structure to limit the table size. The setting of sub-frame size should also be seriously considered. Referring to our previous works [28], [29], we recommend sub-frame size as listed in the Tab. 1.

TABLE 1  
THE RECOMMENDATION SETTING OF  $F_{sub}$

$F$	8~16	32~64	128~256	512~1024	>1024
$F_{sub}$	4	8	16	32	64

### 3.3 Individual Identification Phase

After the cardinality estimation phase, the reader can obtain an approximate estimation of the tag cardinality during its coverage range. Unlike the conventional DFSA algorithm, by dynamically varying the frame size to iteratively identify the remaining tags, the proposed OP-DFSA divides the remaining tag set into  $N$  (where  $N$  is the estimated tag cardinality) subsets according to the estimated cardinality and then conducts individual identification phase on each subset. It is noted that these subsets can be divided into three categories according to the number of tags they contain. The reader needs to mark collided subsets and then conducts individual identification phase on each collided subset. After all collided subsets are successfully identified in sequence, the whole identification process ends. In partitioning based identification phase, the individual identification phase (IIP) on each collided subset is a key component. The details of IIP is described in Fig. 3. In IIP, the reader always starts an identification round with an initial frame size of 2. The initial value of  $N_{id}$  is 0. The reader firstly triggers the first slot and judges its responding status. If an empty slot is detected, the reader will immediately end current identification round. If a collision slot is detected, the reader will trigger the second slot. If a singleton slot is detected, the reader will identify the tag and increase the value of  $N_{id}$  by one.  $N_{id}$  means the number of identified tags in a subset. Only when  $N_{id} \geq 1$ , the reader will continue to trigger the second slot. Otherwise, the reader will end current round. The above identification process will be repeated until no collision occurs. Although the identification process of IIP is very different from the conventional DFSA, the commands used in collision arbitration are same, hence IIP will not bring in extra cost compared to the conventional DFSA. In the IIP phase of the proposed OP-DFSA, the reader needs to terminate the identification round frequently because it adopts the slot-by-slot termination mechanism, which is similar to the those methods used in FEIA [24], ILCM-SbS [27], and DS-MAP algorithm [29]. With the introduction of slot-by-slot termination mechanism, the performance becomes more convergent. We will verify it in the performance evaluation section.

It is noted that the existing EPC C1 Gen2 anti-collision mechanism does not support partitioning operation, thus we made the following modification. For one thing, the reader needs to add extra custom commands to support the functionality of OP-DFSA. For another, the tag needs to add a counter to record slot index. The EPC C1 Gen2 specifies that the reader and tags can use custom commands in accordance with the specification [37]. For the reader, it does not need to change the original hardware circuit. For a tag, the added extra counter is negligible relative to the overall circuit scale of modern tags [40]. Thus, these modifications are based on the scope of changes allowed by existing EPC C1 Gen2 standard and hardware circuit and

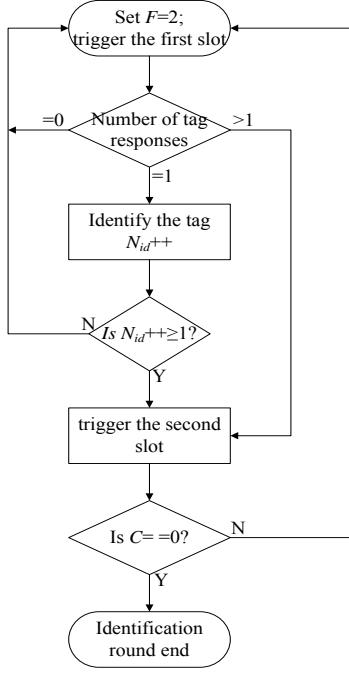


Fig. 3. The flowchart of the IIP process

make worthwhile contribution to significant performance improvement.

#### 4 PERFORMANCE ANALYSIS

In this section, we analyze the slot efficiency, the total slots to identify all tags in OP-DFSA. Herein, the total slots is calculated as total sum of empty slots, singleton slots and collision slots. We first derive the slot efficiency of IIP and then utilize the results of IIP to derive the performance of OP-DFSA.

##### 4.1 Performance Analysis of the IIP Process

Beginning with the simplest cases when the tag number is 2 and 3, we use the induction method to obtain the close-form formula of the slot efficiency for the IIP. Assume there are  $n$  tags in the reader vicinity waiting to be identified, the required number of slots to identify all tags is  $N_n$ . Then the slot efficiency is defined as

$$U_n = \frac{n}{E(N_n)} \quad (6)$$

where  $E(*)$  denotes the function expectation.

Obviously, the identification problem of RFID anti-collision can be viewed as placing  $n$  balls (tags) in  $F$  boxes. For  $n = F = 2$ , the reader will observe four possible cases.

$$\begin{cases} S1 = \{AA, \text{ two tags choose the first slot} \} \\ S2 = \{AB, \text{ two tags choose the different slot} \} \\ S3 = \{BA, \text{ two tags choose the different slot} \} \\ S4 = \{BB, \text{ two tags choose the second slot} \} \end{cases} \quad (7)$$

herein  $A$  and  $B$  can be viewed as the first and second slot, respectively. Therefore, the probability distribution of the above four cases can be listed as

$$\begin{cases} AA & \text{probability } 1/4 & \text{required slots } 2 + N_2 \\ AB, BA & \text{probability } 1/2 & \text{required slots } 2 \\ BB & \text{probability } 1/4 & \text{required slots } 1 + N_2 \end{cases} \quad (8)$$

Then we can have

$$\begin{aligned} E(N_2) &= \frac{1}{4}(2 + E(N_2)) + 2 \times \frac{1}{2} + \frac{1}{4}(1 + E(N_2)) \\ &= 1 + \frac{1}{4}(3 + 2 \times E(N_2)) \\ &\Rightarrow E(N_2) = 3.5 \end{aligned} \quad (9)$$

Therefore, the slot efficiency of the IIP process to identify two tags can be calculated as

$$U_2 = \frac{2}{3.5} = 0.5714 \quad (10)$$

For  $n = 3$ ,  $F = 2$ , the reader can observe eight possible cases, and the probability distribution of them can be expressed as

$$\begin{cases} AAA & \text{probability } 1/8 & \text{required slots } 2 + N_3 \\ ABB, BAB, BBA & \text{probability } 3/8 & \text{required slots } 1 + N_2 \\ AAB, BAA, ABA & \text{probability } 3/8 & \text{required slots } 2 + N_2 \\ BBB & \text{probability } 1/8 & \text{required slots } 1 + N_3 \end{cases} \quad (11)$$

According to (9) and (11), we can have

$$\begin{aligned} E(N_3) &= \frac{1}{8}(2 \times E(N_3) + 3) + \frac{3}{8}(2 \times E(N_2) + 3) \\ &\Rightarrow E(N_3) = 6 \end{aligned} \quad (12)$$

Then the slot efficiency of IIP to identify three tags is calculated as

$$U_3 = \frac{3}{6} = 0.5 \quad (13)$$

Now, we utilize the introduced method to derive the slot efficiency for the IIP.

**Theorem 1.** Let  $n$  denotes the cardinality of tag population within the reader's coverage,  $N_n$  denotes the total slot number consumed to identify these  $n$  ( $n \geq 3$ ) tags, the slot efficiency of the IIP  $U_n^{IIP}$  can be deduced as

$$U_n^{IIP} = \frac{2 \cdot n^2}{2n \cdot E(N_{n-1}) + 2^{n+1} - 1} \quad (14)$$

*Proof:* considering  $n$  tags, there are  $2^n$  cases after the broadcasting of the Query command, the corresponding distribution is expressed as follows:

$$\begin{cases} AA \dots A & \text{probability } 1/2^n & \text{required slots } 2 + N_n \\ \underbrace{a_1 a_2 \dots a_n}_{\sum_{i=1}^n a_i = x \cdot A + y \cdot B} & \text{probability } n/2^n & \text{required slots } 2 + N_{n-1} \\ \underbrace{a_1 a_2 \dots a_n}_{\substack{\sum_{i=1}^n a_i = x \cdot A + y \cdot B \\ x+y=n, x=1, y=n-1}} & \text{probability } C_n^x/2^n & \text{required slots } 2 + N_n \\ \underbrace{a_1 a_2 \dots a_n}_{\substack{\sum_{i=1}^n a_i = x \cdot A + y \cdot B \\ x+y=n, x \geq 2, y \leq n-2}} & \dots & \dots \\ \underbrace{a_1 a_2 \dots a_n}_{\substack{\sum_{i=1}^n a_i = x \cdot A + y \cdot B \\ x+y=n, x=n-1, y=1}} & \text{probability } C_n^{n-1}/2^n & \text{required slots } 2 + N_{n-1} \\ BB \dots B & \text{probability } 1/2^n & \text{required slots } 1 + N_n \end{cases} \quad (15)$$

where  $C_n^x$  denotes choosing  $x$  from  $n$ . From (15), we can have

$$\begin{aligned} E(N_n) &= \frac{1}{2^n} (3 + 2 \times E(N_n)) + \frac{n}{2^n} (2 \times E(N_{n-1}) + 4) \\ &\quad + \sum_{x=2}^{n-2} \frac{C_n^x}{2^n} (E(N_n) + 2) \\ \Rightarrow E(N_n) &= \frac{2n \cdot E(N_{n-1}) + 2^{n+1} - 1}{2n} \end{aligned} \quad (16)$$

According to (6) and (16), the theorem 1 can be yielded.  $\square$

Fig. 4 show the comparison between simulation and theoretical results of IIP process in slot efficiency. As can be seen, the analytical results are highly accurate and closed to the simulations. As also can be observed in Fig. 4, the IIP can achieve higher slot efficiency with an initialized frame size of 2 compared to the conventional DFSA. Especially when the tag number is 2, the attainable slot efficiency of IIP is 0.5714 which is much greater than that of the conventional DFSA. When the frame size is accurately configured, the number of tags involved in most of collision slots is between 2 to 4. Hence, it is foreseeable that the IIP brings a significant performance boost when the tag set is divided into several subsets.

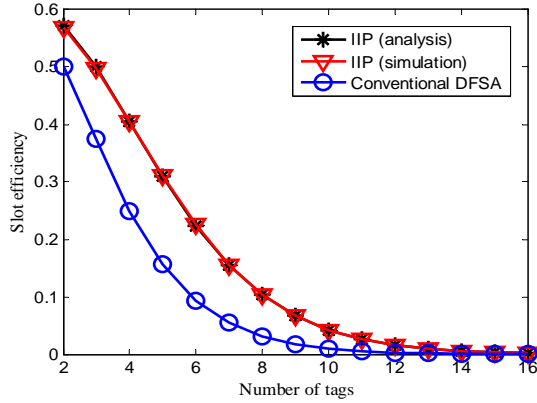


Fig. 4. The comparison between simulation result and theoretical value of slot efficiency

## 4.2 Performance Analysis of OP-DFSA

In this subsection, we analyze the total tag number for identifying all tags in OP-DFSA, and then analyze the slot efficiency in OP-DFSA by using the above analytical results.

**Theorem 2.** Let  $N_n^{OP-DFSA}$  denotes the number of slots consumed by OP-DFSA to identify  $n$  tags, the expected slot number consumed by OP-DFSA algorithm to identify  $n$  tags is

$$E(N_n^{OP-DFSA}) \approx 2.22n \quad (17)$$

*Proof:* Let  $B_r$  ( $r = 2, \dots, n$ ) as the number of subsets containing  $r$  tags,  $N_r^{IIP}$  denotes the expected number of slots to identify  $r$  tags by IIP. Given an initial frame size  $F$ , for each subset, the fill level of  $r$  tags allocated in the subset is described by a binomial distribution with  $1/F$  occupied probability:

$$P_r = C_n^r \left( \frac{1}{F} \right)^r \left( 1 - \frac{1}{F} \right)^{n-r} \quad (18)$$

So the expectation of  $B_r$  can be written as

$$E(B_r) = F \cdot P_r = F \cdot C_n^r \left( \frac{1}{F} \right)^r \left( 1 - \frac{1}{F} \right)^{n-r} \quad (19)$$

Thus, the expectation of  $N_n^{OP-DFSA}$  can be calculated as

$$E(N_n^{OP-DFSA}) = F + \sum_{r=2}^n E(B_r) \cdot E(N_r^{IIP}) \quad (20)$$

When  $F = n$ , OP-DFSA algorithm consumes the least number of slots to identify  $n$  tags. In this case, the total number of slots is optimal. When  $F = n \rightarrow \infty$ , the Eq. (19) can be further expressed as

$$E(B_r) |_{F=n \rightarrow \infty} = \frac{F e^{-1}}{r!} \quad (21)$$

Therefore, according to Theorem 1 and Eq. (21), the optimal number of slots consumed by OP-DFSA algorithm to identify  $n$  tags is

$$\begin{aligned} E(N_n^{OP-DFSA}) &= E(N_n^{OP-DFSA}) |_{F=n \rightarrow \infty} \\ &\approx F + F \sum_{r=2}^n \frac{E(N_r^{IIP})}{r! e} \approx 2.22n \end{aligned} \quad (22)$$

$\square$

**Theorem 3.** The optimal slot efficiency of OP-DFSA is

$$U_{OP-DFSA}^* \approx 0.451 \quad (23)$$

*Proof:* From Theorem 2 and Eq. (6), we have

$$U_{OP-DFSA}^* \approx \frac{n}{2.22n} \approx 0.451 \quad (24)$$

Therefore, Theorem 3 can be yielded.  $\square$

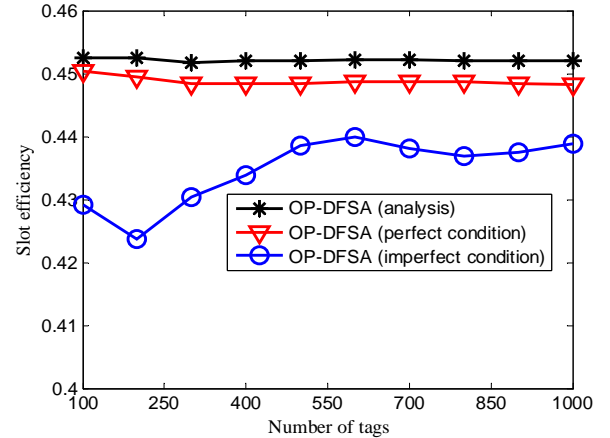


Fig. 5. Comparison of analysis and simulation result for the slot efficiency

It is noted that theorem 3 reveals the slot efficiency threshold of OP-DFSA under perfect condition (the number of tags can be accurately estimate with no error). Since several slots will be consumed in the practical estimation process, the slot efficiency of OP-DFSA is lower than the upper bound. We can verify the effectiveness and reliability of the proposed solution under imperfect conditions through simulations. Fig. 5 provides simulation and theoretical results of OP-DFSA in terms of slot efficiency. The



simulation is conducted through exhaustive Monte-Carlo with 2000 iterations. In the theoretical analysis,  $F = n$  can take any value greater than zero, however, the frame size is limited to  $2^Q$  ( $Q$  is an integer from 0 to 15) in the simulations, so the simulation results will be slightly different from the theoretical results. As can be observed, the simulation results under perfect condition (the tag number is known to the reader) is still very close to the theoretical value, which proves that the theoretical analysis is highly accurate and effective. As also can be found in Fig. 5, the OP-DFSA based LUT estimation can achieve 96% of the optimal performance, which further verifies the effectiveness of the proposed estimation strategy.

## 5 SIMULATION RESULTS

### 5.1 Simulation Setup

In this section, we compared the proposed OP-DFSA with existing state-of-the-art solutions over extensive Monte Carlo simulations. Simulation scenarios with a reader and a various number of tags have been evaluated using MATLAB R2012b, where the tags are uniformly distributed in the reader vicinity so that all tags can receive the reader's command. In our simulations, the sparse mode refers to the number of tags from 5 to 95, and the dense mode refers to the number of tags from 100 to 1000. All the simulation results that we report in this paper were performed in the Lenovo desktop with Intel i5-4590 CPU and 8GB RAM. To reduce the randomness and ensure the convergence, the simulation results are averaged over 2000 iterations [41], [42].

To analyze the algorithm performance, we focus on three metrics: 1) slot efficiency as defined in section I, 2) the number of different types of slots, 3) time efficiency, defined as the time taken to sequentially obtain all IDs divided by the total time required to identify all tags, and 4) tag identification rate, defined as the number of tags that the reader can identify per second.

For each metric, we compare the performance of OP-DFSA with that for the best prior UHF RFID compliant algorithm in the corresponding category of TS-based, Aloha-based, and hybrid. Note that the only prior UHF RFID compliant TS-based tag reading algorithm is PSR [18], and the only prior UHF RFID compliant hybrid tag reading algorithm is ABTSA [23]. There are three prior UHF RFID compliant Aloha-based tag reading algorithms: MAP [10], EACAEA [25], and Q-algorithm [37].

### 5.2 Results on Numerous Metrics

#### 5.2.1 Slot efficiency

OP-DFSA outperforms all other algorithms and achieves nearly the optimal 88.2% slot efficiency under sparse mode. OP-DFSA also outperforms all other algorithms and achieves nearly the optimal 96.4% slot efficiency under dense mode. Fig. 6 (a) compares slot efficiency of various algorithms where the tag number is from 5 to 95. The frame length is initialized as 64. For MAP and EACAEA, their highest slot efficiency can be achieved when the tag number is around the frame size of 64. Since the frame size adjustment strategies of these two algorithms are based on a single estimation, its performance

is subject from the estimation accuracy. When the actual tag number approaches the frame size, they can achieve an accurate estimation and hence obtain a good performance. Conversely, their slot efficiency drops dramatically when the number of tags is greater than the frame size. Compared to MAP and EACAEA, Q-algorithm and Impinj adopt in-frame adjustment strategy which allows identification round to be terminated in any slot of current frame, thus they can maintain more stable performance. However, limited by the framework of conventional DFSA algorithm, the slot efficiency of above protocols is below 0.368. As a contrary, ds-DFSA, PSR and OP-DFSA can provide more higher slot efficiency, they peak at 0.4221, 0.4167, and 0.4337, respectively. The PSR introduces a parallel binary splitting strategy to decrease the number of collision slots and hence to improve the slot efficiency. Since the PSR is not an Aloha-based solution, its performance will not be affected by frame size. The ds-DFSA adopts the divide-and-conquer policy for each collided slots to improve the slot efficiency. However, no improved identification strategy is designed for each collided slot in ds-DFSA. Benefiting from the estimation and IIP, the proposed OP-DFSA achieves the best average slot efficiency. Fig. 6 (b) presents the slot efficiency when the tag number ranges from 100 to 1000. The initial frame size is also set to 64. By comparing both Fig. 6 (a) and (b), most of approaches show discrepant performance. For example, the average slot efficiency of MAP is lower than that of EACAEA when the tag number is from 5 to 95. However, the situation reverses when the tag number ranges between 100 to 1000. The average slot efficiency of PSR is lower than that of ds-DFSA when the tag number is from 5 to 95. When the tag number is between 100 to 1000, the average slot efficiency of PSR is slight higher than that of ds-DFSA. The OP-DFSA always achieves the highest average slot efficiency regardless of the number of tags. Specifically, it peaks at 0.4405 of slot efficiency when the tag number from 100 to 1000.

#### 5.2.2 The number of different types of slots

As concluded in the previous works [27], [28], the slot efficiency is ineffective to evaluate the actual performance of anti-collision approaches because it assumes the time interval of different types of slots are equal. In addition, the number of different types of time slots varies from algorithm to algorithm.

OP-DFSA reduces the total number of slots of the best prior UHF RFID compliant TS-based, Aloha-based, and hybrid algorithms by an average of 6.25%, 17.2%, and 8.4%, respectively, under sparse mode. Meanwhile, OP-DFSA reduces the number of collision slots of the best prior UHF RFID compliant TS-based, Aloha-based, and hybrid algorithms by an average of 35.6%, 14.7%, and 32.6%, respectively. Fig. 7 illustrates the number of different types of slots of various algorithms when the tag number from 5 to 95. Fig. 7 (a) gives the total number of slots for identifying all tags when  $5 \leq n \leq 95$ . Similar to the results for slot efficiency in Fig. 7 (a), the proposed OP-DFSA consumes the least number of slots to identify the tags. As further observed in Fig. 7 (b) and Fig. 7 (c), the OP-DFSA consumes the second smallest number of collision slots and empty slots. It also indicates the proposed OP-DFSA will consume the shorter time to identify all tags due to the fact that a collision slot has a longer time interval than of an empty slot. In PSR and ABTSA, the tag ID is used



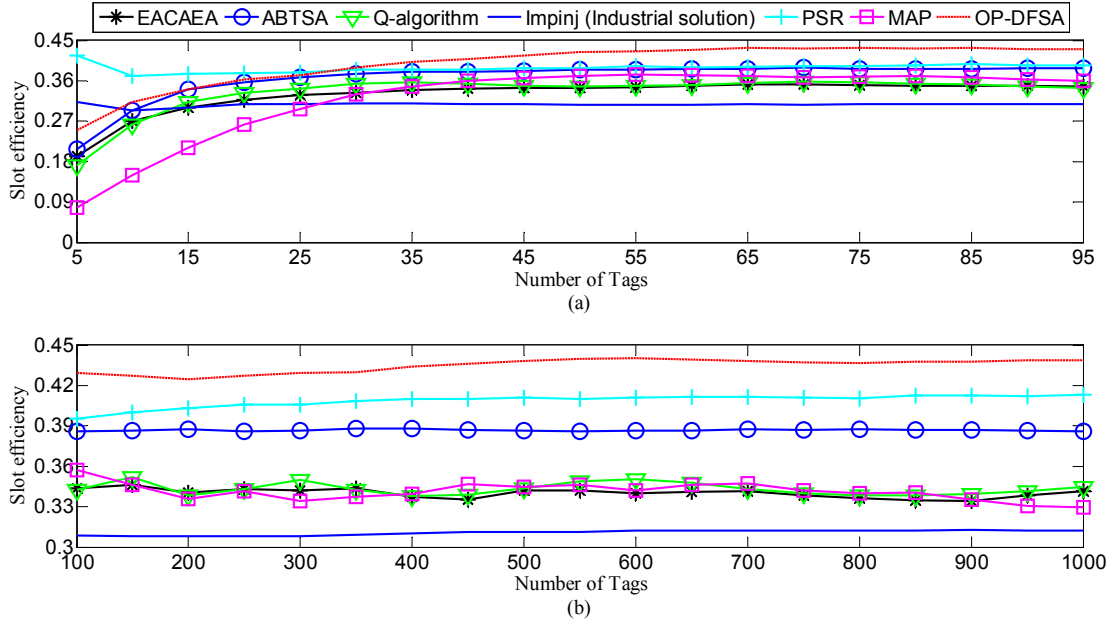


Fig. 6. Comparison of slot efficiency of various algorithms: (a) sparse mode (b) dense mode

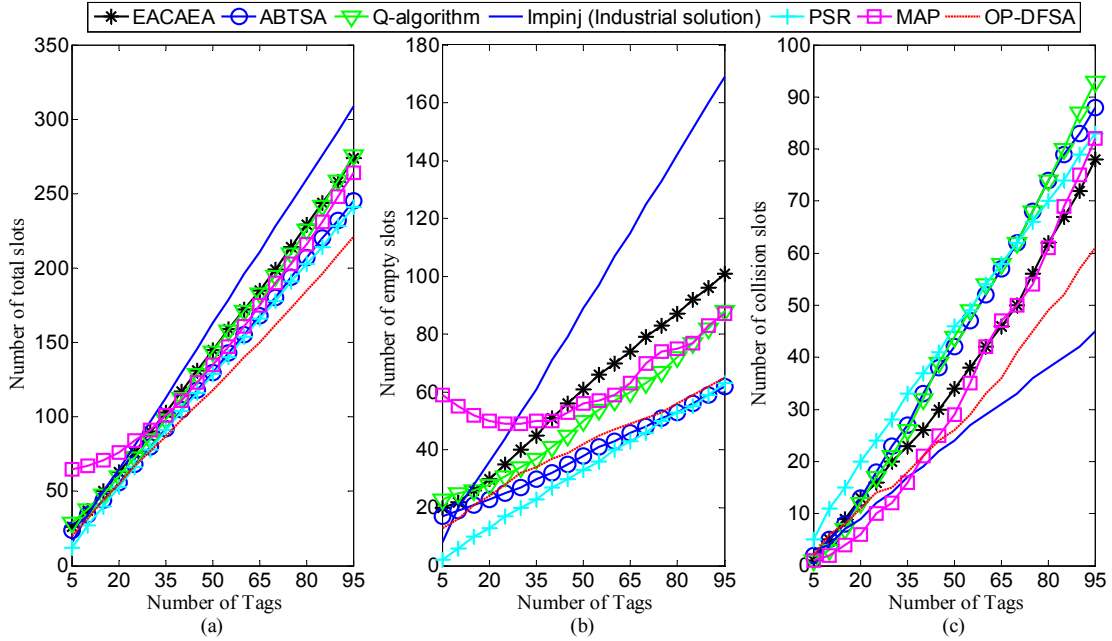


Fig. 7. Comparison of time slots consumption under sparse mode

for collision arbitration. The time duration of a collision slot is equal to that of a singleton slot. Therefore, they potentially have a potential low time efficiency compared to the other Aloha-based algorithm including EACAEA, ds-DFSA and OP-DFSA. Although the number of collision slots consumed by OP-DFSA is slightly more than Impinj, its time efficiency will be higher than Impinj because the total number of slots is smaller.

OP-DFSA reduces the total number of slots of the best prior UHF RFID compliant TS-based, Aloha-based, and hybrid algorithms by an average of 5.97%, 22.3%, and 11.5%, respectively, under dense mode. Meanwhile, OP-DFSA reduces the number of

collision slots of the best prior UHF RFID compliant TS-based, Aloha-based, and hybrid algorithms by an average of 23.8%, 30.1%, and 42.2%, respectively. Fig. 8 compares the number of different types of slots of various algorithms when the tag number from 100 to 1000. Similar results in Fig. 7 can be observed in Fig. 8. The primary difference is that the Q-algorithm consumes the most number of collision slots when  $5 \leq n \leq 95$ , however it consumes the second least number of collision slots when  $100 \leq n \leq 1000$ . Regardless of the number of tags, the proposed OP-DFSA always consumes the least number of total slots and the second smallest number of collision slots. According to

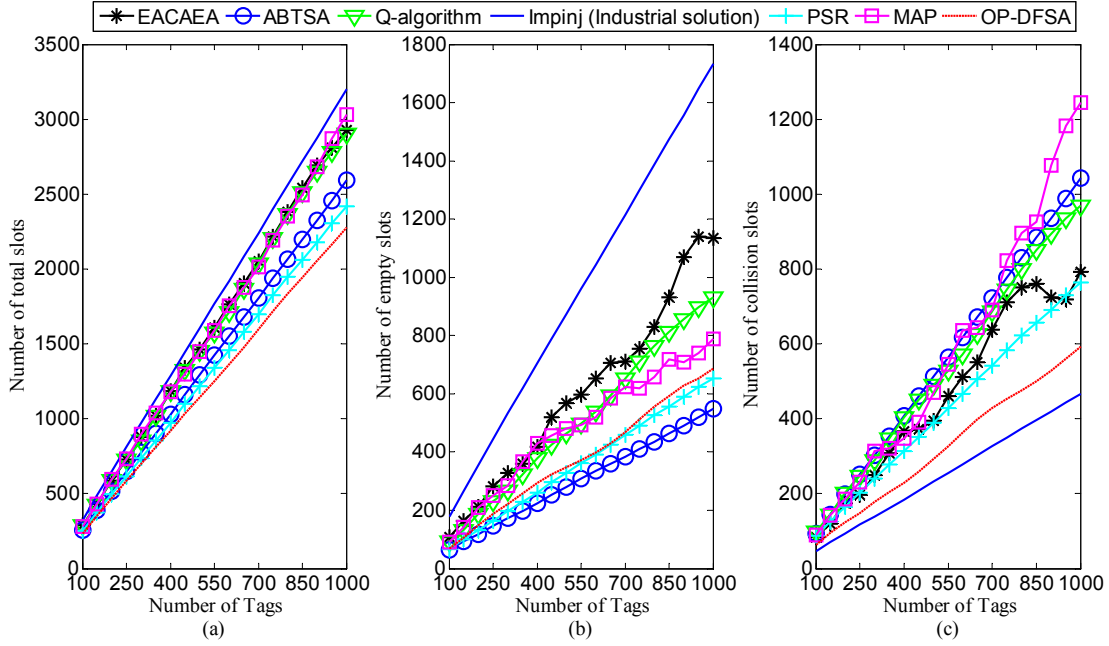


Fig. 8. Comparison of time slots consumption under dense mode

the analysis above, it can potentially achieve the best time efficiency. Both Fig. 7 and Fig. 8 reflect the difference in the slot distribution of various algorithm. Therefore, to better evaluate the performance of anti-collision algorithms, the time efficiency is taken into account in the simulations. Referring to [13], [16], [28], [42], the time efficiency is defined as

$$\eta = \frac{n \cdot T_{EPC}}{n \cdot T_S + N_E \cdot T_E + N_C \cdot T_C} \quad (25)$$

where  $T_{EPC}$  denotes the time interval required for transmitting a tag's EPC.  $n$ ,  $N_E$ , and  $N_C$  denote the number of singleton slots, empty slots, and collision slots, respectively.  $T_S$ ,  $T_E$ , and  $T_C$  represent the corresponding time intervals of above three types of slots, and they are measured by the reader during the identification process. According to link timing described in Fig. 1, we have

$$T_S = T_{cmd} + 2(T_1 + T_2) + T_{RN16} + T_{ACK} + T_{EPC} \quad (26)$$

$$T_E = T_{cmd} + T_1 + T_3 \quad (27)$$

$$T_C = T_{cmd} + T_1 + T_2 + T_{RN16} \quad (28)$$

where  $T_{cmd}$  is the time duration taken by the anti-collision command transmitted by the reader, which can be Query, QueryAdj, QueryRep, etc [28].

### 5.2.3 Time efficiency

OP-DFSA improves the time efficiency of the best prior UHF RFID compliant TS-based, Aloha-based, and hybrid algorithms by an average of 22.4%, 5.02%, and 14.5%, respectively, under sparse mode. OP-DFSA improves the time efficiency of the best prior UHF RFID compliant TS-based, Aloha-based, and hybrid algorithms by an average of 16.2%, 7.45%, and 22.1%, respectively, under dense mode. Fig. 9 illustrate the time efficiency of

TABLE 2  
THE TIME PARAMETERS USED IN MATLAB SIMULATIONS

Parameters	Values
Frequency (MHz)	912.5
BLF (kHz)	40
Modulation	DSB-ASK
RTcal ( $\mu$ s)	75
TRcal ( $\mu$ s)	200
DR	8
T->R Modulation	FM0
TRExt	1
Tari ( $\mu$ s)	25

various algorithms. The time parameters used to evaluate the time efficiency are listed in Tab. 2. Fig. 9 (a) compares the time efficiency of various algorithms when  $5 \leq n \leq 95$ . As analyzed in the previous content, the time efficiency is highly affected by the time duration and number of collision slots. Although the total number of slots consumed by Q-algorithm is less than Impinj, the time efficiency of Impinj is higher than Q-algorithm because Impinj algorithm consumes fewer collision slots. The observed results also verify that the PSR and ABTSA have a lower time efficiency than Aloha-based algorithms. As also can be observed in Fig. 9 (a), the time efficiency of MAP, EACAEA, and Impinj is very close because they have an approximate number of collision slots when  $n$  is below 100. As the tag number increases, the gap between the number of collision slots of various algorithms increases. Under the same conditions as the total number of slots, the fewer number of collision slots, the higher the time efficiency. As can be found in Fig. 9 (b), the time efficiency of MAP is lower than that of EACAEA and Impinj due to its large number of collision slots. Since the number of collision slots of ABTSA increases dramatically when the tag number is above 100, its time efficiency becomes lower than PSR. On the contrary, since

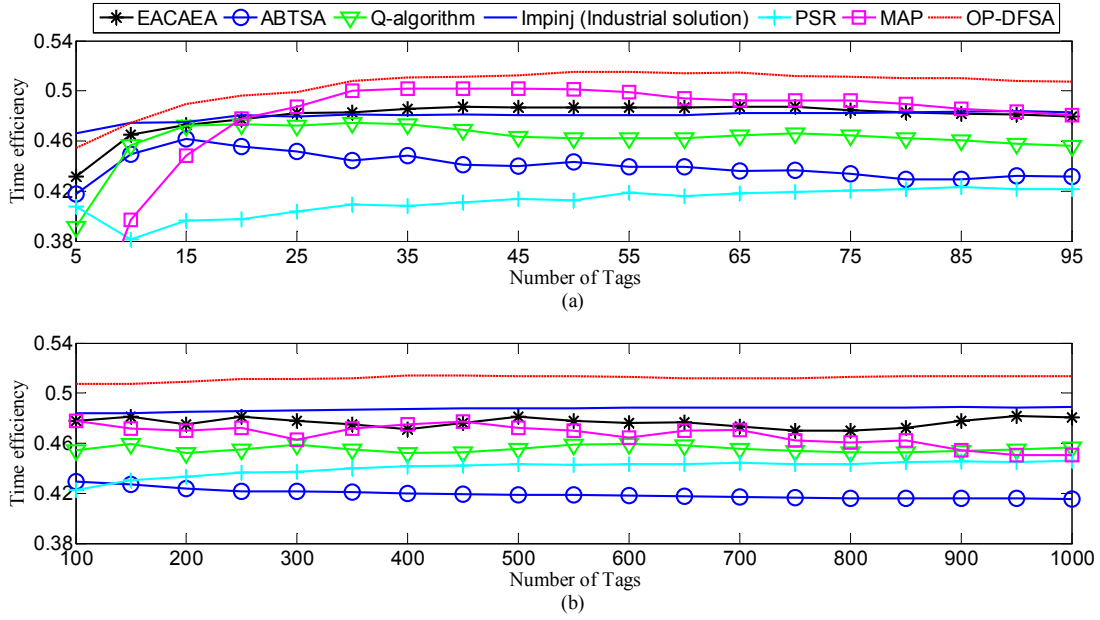


Fig. 9. Comparison of time efficiency of various algorithms: (a) sparse mode (b) dense mode

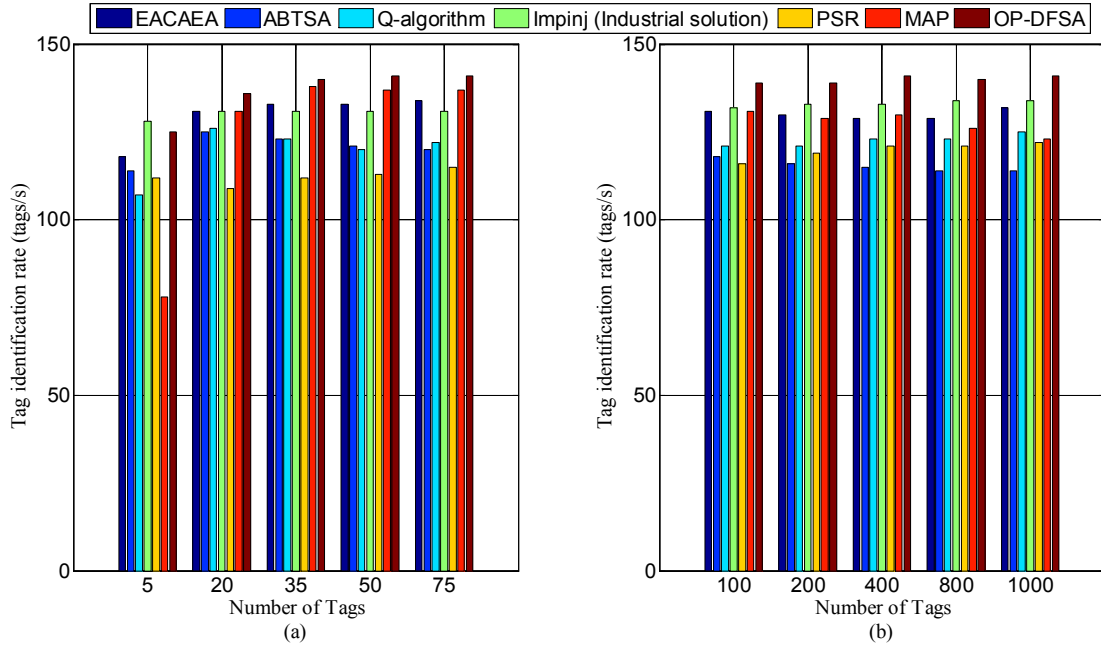


Fig. 10. Comparison of tag identification rate: (a) sparse mode (b) dense mode

the proposed OP-DFSA holds both the least number of total slots and collision slots, it achieves the best performances in terms of both slot efficiency and time efficiency.

#### 5.2.4 Tag identification rate

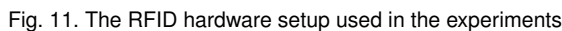
OP-DFSA improves the tag identification rate of the best prior UHF RFID compliant TS-based, Aloha-based, and hybrid algorithms by an average of 21.8%, 5.24%, and 13.3%, respectively, under sparse mode. OP-DFSA improves the time efficiency of the best prior UHF RFID compliant TS-based, Aloha-based, and hybrid algorithms by an average of 16.9%, 7.69%, and 21.3%, respectively, under dense mode. Existing commercial or

enterprise-level RFID systems focus on the tag identification rate of the readers. The tag identification rate is defined as the number of tags can be successfully identified per second. The comparison of tag identification rate of various algorithms is shown in Fig. 10, the frame size is also initialized as 64. A similar trend as in the time efficiency can be observed here. As can be observed in Fig. 10 (a), all algorithms perform the lowest identification rate when the number of tags is equal to 5 except PSR and Q-algorithm. That is because the Aloha-based algorithms consume a lot of empty slots when the initialized frame size is much greater than the tag number, especially for the MAP algorithm, whose estimation is

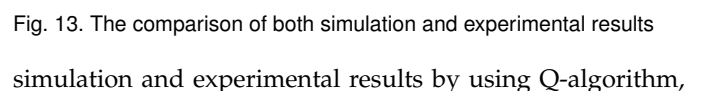
Figure 1 consists of three vertically stacked panels sharing a common horizontal axis labeled  $n$ , ranging from 0 to 100. The top panel shows a probability distribution  $P_n(t)$  on the vertical axis, with a dashed red line indicating a linear increase in the peak position. The middle panel shows a probability distribution  $P_n(t)$  on the vertical axis, with a dashed red line indicating a linear increase in the peak position. The bottom panel shows a probability distribution  $P_n(t)$  on the vertical axis, with a dashed red line indicating a linear increase in the peak position. Labels include 'collision slot', 'singleton slot', and 'empty slot'.

and USB. The custom tag is programmed to support the custom commands transmitted from the reader. The entire hardware environment used for experiments is captured in Fig. 11, which includes a reader module, power supply, custom tags, commercial tags, an antenna, an oscilloscope, and a computer. The link parameters configured for radio frequency communication between the reader and tags are consistent with the simulation parameters listed in Tab. 2. To consider physical factors such as noise and multi-path effects, we placed the tags in the foam board which was placed on a small trailer. And then we moved the trailer along with the track to pass in front of the reader antenna.

Before the performance test of the anti-collision algorithms, we first capture the waveform through the oscilloscope to verify the function of the reader to detect the responses from custom tags. Fig. 12 shows the waveform captured by the oscilloscope during a multi-tag identification process, from which the empty, collision and singleton slot can be clearly detected by the reader. Fig. 13 shows both



To further evaluate the performance of the proposed OP-DFSA algorithm in a practical UHF RFID system, we conduct experiments with a testbed in an indoor environment. The prototype of OP-DFSA is implemented in an active reader and programmable custom tags. The reader is equipped with ARM Cortex A9 processor, which is a 32-bit reduced instruction set (RISC) processor with a maximum operating frequency of 1 GHz and an off-chip memory 512M to ensure high speed and stable operation of the program. The enrich interfaces include UART, JTAG, ETH,



Impinj algorithm and OP-DFSA algorithm to identify the same batch tags in the same time period under low data rate mode. As can be observed from Fig. 13 (a), the proposed OP-DFSA reduces the identification time (defined as the total time required to identify all tags) by 7.18% and 1.75% with 20 tags and improves average identification rate (defined as the number of tags can be identified per unit time) by 5.8% and 2.82% compared with standard Q-algorithm and Impinj industrial solution illustrated in Fig. 13 (b), respectively. As can be found from the Fig. 13, the measured performance has a certain difference compared with the numerical results. The potential reasons can be analyzed as follows. Since the measurements are performed in a mobile scenario, we consider that the difference arises due to influence of radio effects. Under a mobile scenario, some tags may not be successfully decoded, since its received power is less than required tag sensitivity (defined as the minimal power level supports). The root cause is multi-path effects and signal attenuation caused by walls or other obstacles. It can be observed that in the same scenario, the proposed OP-DFSA still outperforms Q-algorithm and Impinj solution. In addition, since the experiments are carried out in the low-speed mode (i.e., the data rate is only 40 kbps), the performance advantages of the proposed OP-DFSA are not fully reflected. The advantages of OP-DFSA will become more obvious as the number of tags increases and the data rate increases. The observed experiment results also indicate that the performance of all MAC protocols will be affected by radio effects. Finally, because the focus of this paper is on MAC layer, the impact of these radio effects is beyond the scope of our research.

## 7 CONCLUSIONS

In this paper, we make the following three key contributions. First, we formulate the tag identification problem as a partitioning problem and propose an optimal partition based DFSA algorithm for passive UHF RFID systems to maximize reading performance. Unlike conventional DFSA algorithms, the OP-DFSA allows the tags to be partitioned into several subsets, then the reader identifies the individual subsets sequentially. Focusing on the identification of an individual subset, we design an efficient identification mechanism. Second, we propose a new strategy to estimate the tag cardinality. In the estimation process, the result is calculated by maximum likelihood estimator during a sub-frame and pre-saved in a table. Thus, it reduces the computational complexity. Third, we implement the proposed OP-DFSA in a practical RFID system, which includes a fixed reader and 20 custom tags. The experiments indicate that the proposed OP-DFSA is a suitable candidate for the commercial and industrial RFID systems.

## REFERENCES

- [1] L. Zhu and T.-S. P. Yum, "A critical survey and analysis of rfid anti-collision mechanisms," *IEEE Trans. Ind. Informat.*, vol. 49, no. 5, pp. 214–221, 2011.
- [2] K. Finkenzeller, *RFID handbook: fundamentals and applications in contactless smart cards, radio frequency identification and near-field communication*. John Wiley & Sons, 2010.
- [3] J. Su, Z. Sheng, V. C. Leung, and Y. Chen, "Energy efficient tag identification algorithms for rfid: survey, motivation and new design," *IEEE Wireless Commun.*, vol. 26, no. 3, pp. 118–124, 2019.
- [4] P. Yang, W. Wu, M. Moniri, and C. C. Chibelushi, "Efficient object localization using sparsely distributed passive rfid tags," *IEEE Trans. Ind. Electron.*, vol. 60, no. 12, pp. 5914–5924, 2013.
- [5] S. S. Saab and Z. S. Nakad, "A standalone rfid indoor positioning system using passive tags," *IEEE Trans. Ind. Informat.*, vol. 58, no. 5, pp. 1961–1970, 2011.
- [6] R. Das, *RFID forecasts, players and opportunities 2017-2027*. IDTechEx, 2017.
- [7] D. K. Klair, K.-W. Chin, and R. Raad, "A survey and tutorial of rfid anti-collision protocols," *IEEE Commun. Surveys Tuts.*, vol. 12, no. 3, pp. 400–421, 2010.
- [8] M. Bolic, D. Simplot-Ryl, and I. Stojmenovic, *RFID systems: research trends and challenges*. IDTechEx, 2011.
- [9] J. Vales-Alonso, V. Bueno-Delgado, E. Egea-Lopez, F. J. Gonzalez-Castaño, and J. Alcaraz, "Multiframe maximum-likelihood tag estimation for rfid anticollision protocols," *IEEE Trans. Ind. Informat.*, vol. 7, no. 3, pp. 487–496, 2011.
- [10] W.-T. Chen, "An accurate tag estimate method for improving the performance of an rfid anticollision algorithm based on dynamic frame length aloha," *IEEE Trans. Autom. Sci. Eng.*, vol. 6, no. 1, pp. 9–15, 2009.
- [11] B. Knerr, M. Holzer, C. Angerer, and M. Rupp, "Slot-wise maximum likelihood estimation of the tag population size in fsa protocols," *IEEE Trans. Commun.*, vol. 58, no. 2, pp. 578–585, 2010.
- [12] Y. He and X. Wang, "An aloha-based improved anti-collision algorithm for rfid systems," *IEEE Wireless Commun.*, vol. 20, no. 5, pp. 152–158, 2013.
- [13] L. Zhu and T.-S. P. Yum, "The optimal reading strategy for epc gen-2 rfid anti-collision systems," *IEEE Trans. Commun.*, vol. 58, no. 9, pp. 2725–2733, 2010.
- [14] L. Barletta, F. Borgonovo, and M. Cesana, "A formal proof of the optimal frame setting for dynamic-frame aloha with known population size," *IEEE Trans. Inf. Theory*, vol. 60, no. 11, pp. 7221–7230, 2014.
- [15] R. Jayadi, Y.-C. Lai, and C.-C. Lin, "Efficient time-oriented anti-collision protocol for rfid tag identification," *Comput. Commun.*, vol. 112, pp. 141–153, 2017.
- [16] M. Shahzad and A. X. Liu, "Ieee/acm trans. netw." *Probabilistic optimal tree hopping for RFID identification*, vol. 23, no. 3, pp. 796–809, 2015.
- [17] J. Su, Z. Sheng, L. Xie, G. Li, and A. X. Liu, "Fast splitting based tag identification algorithm for anti-collision in uhf rfid system," *IEEE Trans. Commun.*, vol. 67, no. 3, pp. 2527–2538, 2019.
- [18] H. Guo, C. He, N. Wang, and M. Bolic, "PSR: A novel high-efficiency and easy-to-implement parallel algorithm for anticollision in rfid systems," *IEEE Trans. Ind. Informat.*, vol. 12, no. 3, pp. 1134–1145, 2016.
- [19] C. Floerkemeier, "Transmission control scheme for fast rfid object identification," in *Proc. 4th Annu. IEEE Int. Conf. Pervasive Comput. Workshops*, pp. 457–462, 2006.
- [20] A. Zanella, "Estimating collision set size in framed slotted aloha wireless networks and rfid systems," *IEEE Commun. Lett.*, vol. 16, no. 3, pp. 300–303, 2012.
- [21] L. Zhang, W. Xiang, X. Tang, Q. Li, and Q. Yan, "A time-and energy-aware collision tree protocol for efficient large-scale rfid tag identification," *IEEE Trans. Ind. Informat.*, vol. 14, no. 6, pp. 2406–2417, 2018.
- [22] V. Namboodiri and L. Gao, "Energy-aware tag anticollision protocols for rfid systems," *IEEE Trans. Mobile Comput.*, vol. 9, no. 1, pp. 44–59, 2010.
- [23] H. Wu, Y. Zeng, J. Feng, and Y. Gu, "Binary tree slotted aloha for passive rfid tag anticollision," *IEEE Trans. Parallel Distrib. Syst.*, vol. 24, no. 1, pp. 19–31, 2013.
- [24] W.-T. Chen, "A feasible and easy-to-implement anticollision algorithm for the epcglobal uhf class-1 generation-2 rfid protocol," *IEEE Trans. Autom. Sci. Eng.*, vol. 11, no. 2, pp. 485–491, 2014.
- [25] W.-T. Chen, "Optimal frame length analysis and an efficient anti-collision algorithm with early adjustment of frame length for rfid systems," *IEEE Trans. Veh. Technol.*, vol. 65, no. 5, pp. 3342–3348, 2016.
- [26] P. Šolić, J. Radić, and N. Rožić, "Energy efficient tag estimation method for aloha-based rfid systems," *IEEE Sensors J.*, vol. 14, no. 10, pp. 3637–3647, 2014.



- [27] P. Šolić, J. Radić, and N. Rožić, "Early frame break policy for aloha-based rfid systems," *IEEE Trans. Autom. Sci. Eng.*, vol. 13, no. 2, pp. 876–881, 2016.
- [28] J. Su, Z. Sheng, D. Hong, and V. Leung, "An efficient sub-frame based tag identification algorithm for uhf rfid systems," in *IEEE Int. Conf. Commun. (ICC 2016)*, pp. 1–6, 2016.
- [29] Y. Chen, J. Su, and W. Yi, "An efficient and easy-to-implement tag identification algorithm for uhf rfid systems," *IEEE Commun. Lett.*, vol. 21, no. 7, pp. 1509–1512, 2017.
- [30] J. Su, Z. Sheng, D. Hong, and G. Wen, "An effective frame breaking policy for dynamic framed slotted aloha in rfid," *IEEE Commun. Lett.*, vol. 20, no. 4, pp. 692–695, 2016.
- [31] C. Law, K. Lee, and K.-Y. Siu, "Efficient memoryless protocol for tag identification," in *Proc. 4th Int. Workshop Discrete Algor. Methods Mobile Comput. Commun.*, pp. 75–84, 2000.
- [32] X. Jia, Q. Feng, and L. Yu, "Stability analysis of an efficient anti-collision protocol for rfid tag identification," *IEEE Trans. Commun.*, vol. 60, no. 8, pp. 2285–2294, 2012.
- [33] L. Pan and H. Wu, "Smart trend-traversal protocol for rfid tag arbitration," *IEEE Trans. Wireless Commun.*, vol. 10, no. 11, pp. 3565–3569, 2011.
- [34] J. Shin, B. Jeon, and D. Yang, "Multiple rfid tags identification with m-ary query tree scheme," *IEEE Commun. Lett.*, vol. 17, no. 3, pp. 604–607, 2013.
- [35] H. Landaluze, A. Perallos, E. Onieva, L. Arjona, and L. Bengtsson, "An energy and identification time decreasing procedure for memoryless rfid tag anticollision protocols," *IEEE Trans. Wireless Commun.*, vol. 15, no. 6, pp. 4234–4247, 2016.
- [36] J. Su, Z. Sheng, G. Wen, and V. C. Leung, "A time efficient tag identification algorithm using dual prefix probe scheme (dpps)," *IEEE Process. Lett.*, vol. 23, no. 3, pp. 386–389, 2016.
- [37] EPCglobal, "EPC radio-frequency identity protocols generation-2 uhf rfid protocol for communications at 860 mhz-960 mhz," *version 2.0.1*, 2013.
- [38] L. Zhang, J. Zhang, and X. Tang, "Assigned tree slotted aloha rfid tag anti-collision protocols," *IEEE Trans. Wireless Commun.*, vol. 12, no. 11, pp. 5493–5505, 2013.
- [39] E. Vahedi, V. W. Wong, I. F. Blake, and R. K. Ward, "Probabilistic analysis and correction of chen's tag estimate method," *IEEE Trans. Autom. Sci. Eng.*, vol. 8, no. 3, pp. 659–663, 2011.
- [40] J. A. Rodríguez-Rodríguez, M. Delgado-Restituto, J. Masuch, A. Rodríguez-Pérez, E. Alarcon, and A. Rodríguez-Vázquez, "An ultralow-power mixed-signal back end for passive sensor uhf rfid transponders," *IEEE Trans. Ind. Electron.*, vol. 59, no. 2, pp. 1310–1322, 2011.
- [41] J. Su, Z. Sheng, L. Xie, G. Li, and A. X. Liu, "Fast splitting based tag identification algorithm for anti-collision in uhf rfid system," *IEEE Trans. Commun.*, vol. 67, no. 3, pp. 2527–2538, 2019.
- [42] X. Liu, B. Xiao, K. Li, A. X. Liu, J. Wu, X. Xie, and H. Qi, "Rfid estimation with blocker tag," *IEEE/ACM Trans. Netw.*, vol. 25, no. 1, pp. 224–237, 2017.



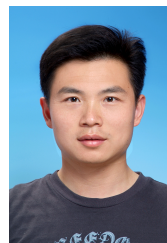
**Jian Su** has been a lecturer in the School of Computer and Software at the Nanjing University of Information Science and Technology since 2017. He received his PhD with distinction in communication and information systems at University of Electronic Science and Technology of China (UESTC) in 2016. He holds a B.S. in Electronic and information engineering from Hankou university and an M.S. in electronic circuit and system from Central China Normal University. His current research interests cover Internet of Things, RFID, and Wireless sensors networking. He is a member of IEEE and a member of ACM.



**Alex X. Liu** received his Ph.D. degree in Computer Science from The University of Texas at Austin in 2006, and is currently an adjunct professor of Qilu University of Technology and a Chief Scientist of the Ant Financial Services Group. Before that, he was a Professor of the Department of Computer Science and Engineering at Michigan State University. He received the IEEE & IFIP William C. Carter Award in 2004, a National Science Foundation CAREER award in 2009, the Michigan State University Withrow Distinguished Scholar (Junior) Award in 2011, and the Michigan State University Withrow Distinguished Scholar (Senior) Award in 2019. He has served as an Editor for IEEE/ACM Transactions on Networking, and he is currently an Associate Editor for IEEE Transactions on Dependable and Secure Computing, IEEE Transactions on Mobile Computing, and an Area Editor for Computer Communications. He has served as the TPC Co-Chair for ICNP 2014 and IFIP Networking 2019. He received Best Paper Awards from SECON-2018, ICNP-2012, SRDS-2012, and LISA-2010. His research interests focus on networking, security, and privacy. He is an IEEE Fellow and an ACM Distinguished Scientist.



**Zhongguo Sheng** has been a senior lecturer in the Department of Engineering and Design at the University of Sussex since 2015. He received his Ph.D. and M.S. with distinction at Imperial College London in 2011 and 2007, respectively, and his B.Sc. from the University of Electronic Science and Technology of China (UESTC) in 2006. His current research interests cover the Internet of Things (IoT), connected vehicles, and cloud/ edge computing.



**Yongrui Chen** is currently an Associate Professor with the School of Electronic, Electrical and Communication Engineering, University of Chinese Academy of Sciences. He has received his M.S degree from Tsinghua University, China in 2007, and Ph.D. degree from University of Chinese Academy of Sciences, China in 2011. His research interests include Internet of Things, wireless and mobile computing, and heterogeneous wireless networks. He is a member of IEEE.